

In presenting the dissertation as a partial fulfillment of the requirements for an advanced degree from the Georgia Institute of Technology, I agree that the Library of the Institute shall make it available for inspection and circulation in accordance with its regulations governing materials of this type. I agree that permission to copy from, or to publish from, this dissertation may be granted by the professor under whose direction it was written, or, in his absence, by the Dean of the Graduate Division when such copying or publication is solely for scholarly purposes and does not involve potential financial gain. It is understood that any copying from, or publication of, this dissertation which involves potential financial gain will not be allowed without written permission.

3/17/65

b

REDUCTION OF THE NONLINEARITY OF VALVING
ARRANGEMENTS INCORPORATING THE VARIABLE JET PUMP

A THESIS

Presented to

The Faculty of the Graduate Division

by

Homer Millard Vernon, Jr.

In Partial Fulfillment

of the Requirements for the Degree

Master of Science in Mechanical Engineering

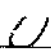
Georgia Institute of Technology

June, 1967

REDUCTION OF THE NONLINEARITY OF VALVING
ARRANGEMENTS INCORPORATING THE VARIABLE JET PUMP

Approved:


Chairman


Date approved by Chairman: May 22, 1967

ACKNOWLEDGMENTS

The author would like to express his sincere appreciation to Dr. Stephen Dickerson for his suggestions and continual help throughout this work. Appreciation is also extended to Dr. John Peatman and Dr. Donaldson McCloy for their services on the thesis reading committee.

A particular thanks is extended to my family whose interest and encouragement has been a constant help, and especially to my father, Homer Vernon, who has been an inspiration throughout my entire college career. A special thanks is needed for my wife, Glenda, who has given me moral support and has contributed in many ways to the completion of this thesis.

Support for the author as well as funds for equipment was provided by a National Science Foundation research grant. These funds were supplemented by funds from the Mechanical Engineering Department.

TABLE OF CONTENTS

	Page
ACKNOWLEDGMENTS.	ii
LIST OF ILLUSTRATIONS.	iv
LIST OF SYMBOLS AND ABBREVIATIONS.	v
SUMMARY.	vii
Chapter	
I. INTRODUCTION.	1
The Variable Jet Pump	
II. STEADY STATE CHARACTERISTICS.	3
The Steady State Tests	
Variable Jet Pump Valve	
Torque Motor	
Instrumentation	
III. DYNAMIC CHARACTERISTICS	8
Theoretical Response	
Actual System Response	
Instrumentation and Equipment	
IV. CONCLUSIONS AND RECOMMENDATIONS	19
APPENDIX	
I. HYDRAULIC SUPPLY SYSTEM	21
II. ILLUSTRATIONS AND GRAPHICAL RESULTS	23
III. CONSTANTS AND DERIVATIONS	32
BIBLIOGRAPHY	39

LIST OF ILLUSTRATIONS

Figure		Page
1.	The Variable Jet Pump Configuration	2
2.	Typical Pressure-flow Curves.	3
3.	Block Diagram for Pressure Compensated Variable Jet Pump	8
4.	Linearized Variable Jet Pump or Variable Orifice Block Diagram	13
5.	Combined Variable Jet Pump Valve Block Diagram.	14
6.	Composite System.	15
7.	Hydraulic Power Supply System	22
8.	Variable Jet Pump Cross Section	24
9.	Two-way Variable Jet Pump Valve Arrangement	25
10.	Variable Jet Pump Valve Characteristics with Torque Motor	26
11.	Variable Jet Pump Valve Characteristics without Torque Motor.	27
12.	Variable Jet Pump Valve Characteristics Without Pressure Compensation	28
13.	Pressure Compensating Spool and Downstream Orifice.	29
14.	Variable Jet Pump Valve Frequency Response.	30
15.	Variable Jet Pump Valve Dynamic Test Arrangement.	31
16.	Torque Motor Frequency Response	34

LIST OF SYMBOLS AND ABBREVIATIONS

A_T	area of variable jet pump throat
d	variable jet pump slider diameter
D	variable jet pump throat diameter
f	normalized force $\frac{F}{K_{TM} (\frac{d}{2})}$
G_{TM}	torque motor current gain
i	normalized input current $\frac{I}{\frac{K_{TM}}{G_{TM}} (\frac{d}{2})}$
K_O	normalized orifice constant
K_{TM}	spring constant of torque motor
p	normalized pressure $\frac{P}{P_S - P_E}$
P_E	exhaust pressure
P_L	load pressure
P_S	supply pressure
P_O	load pressure operating point (a constant)
P_1	upstream load pressure
P_2	downstream load pressure
q	normalized flow $\frac{Q}{A_T \sqrt{\frac{2(P_S - P_E)}{p}}}$
Q_L	load flow

Q_s	supply flow
Q_o	load flow operating point (a constant)
ρ	density
x	normalized variable jet pump slider position $\frac{x}{d/2}$
x_{VJP}	variable jet pump slider position operating point (a constant)
x_{V0}	variable orifice slider position operating point (a constant)
VJP	variable jet pump
$VJPV$	variable jet pump valve

SUMMARY

This thesis continues the investigation of the variable jet pump started by Dr. S. L. Dickerson. In his work Dr. Dickerson developed a workable variable jet pump design and used this model in a four-way control system. He showed that as a modulator of fluid power the variable jet pump would typically halve system power requirements.

This work analyzes a further use of the variable jet pump as a modulated fluid transformer. A two-way servo system incorporating the variable jet pump is developed and tested. This system is designed with pressure compensation to reduce the nonlinearities characteristic of the variable jet pump. Both static and dynamic characteristics are studied and a theoretical analysis is presented. A short discussion is included which suggests further applications of the variable jet pump.

CHAPTER I

INTRODUCTION

A variable fluid transformer in the form of a variable jet pump was developed at the Massachusetts Institute of Technology in the doctoral thesis of Stephen L. Dickerson in 1965 (1). In the above work, Dr. Dickerson showed that power requirements for the variable jet pump controlled servo system were typically one-half that of a spool type servo system. However, the resulting characteristic pressure-flow curves for the variable jet pump valve show a high degree of nonlinearity. The objective of this work is first, to linearize the characteristic curves using a pressure feedback system, and secondly, to determine if the frequency response of the pressure compensated variable jet pump valve is still above acceptable standards.

A two-way pressure control valve was chosen as the test model. Tests were first conducted to show the nonlinearity of the uncompensated variable jet pump valve. Other tests were then conducted to show the linearizing effect of pressure compensation. The dynamic characteristics of the pressure compensated variable jet pump were also determined.

The Variable Jet Pump

The variable jet pump developed in reference (1) is, in principle, a relatively simple device.

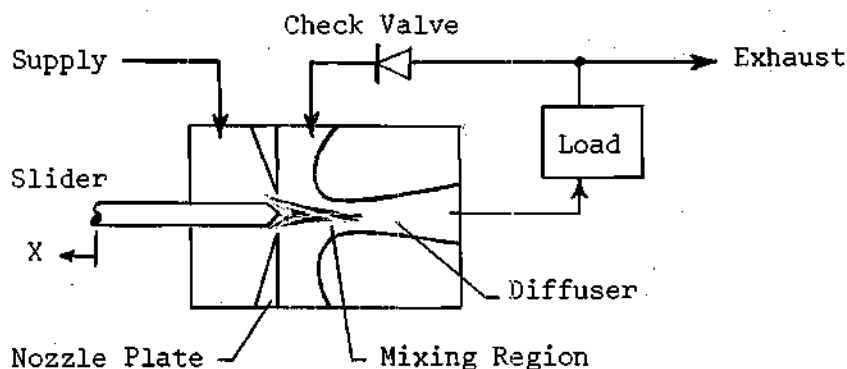


Figure 1. The Variable Jet Pump Configuration

A high velocity jet of fluid enters through an orifice in the nozzle plate from the supply. A slider modulates the jet as it enters a low pressure region. Then the jet and some fluid entrained from the low pressure region enter a mixing region where an exchange of momentum takes place. From the mixing region the fluid streams to the diffuser where the kinetic energy of the mixture is recovered. The variable jet pump and check valve used for this thesis are the identical ones used by Dr. Dickerson (see Figure 8). The test model was constructed by adding pressure compensation, input, and load to the above variable jet pump. The interaction of the variable jet pump with the over-all system will be explained in Chapters II and III.

CHAPTER II

STEADY STATE CHARACTERISTICS

Typically steady state pressure-flow curves for a two-way pressure compensated valve are vertical lines in the positive flow region. When the valve is in operation, a signal input produces a proportional pressure output. Negative pressures can be obtained by means of a driving load, such as an inertia or a falling weight. The slope of the characteristic pressure-flow curves is due to either flow forces in the valve or some spring force tending to position the valve. There is a boundary shown in the example below where the valve is wide open and the pressure can be increased only at a cost of a reduction in the flow.

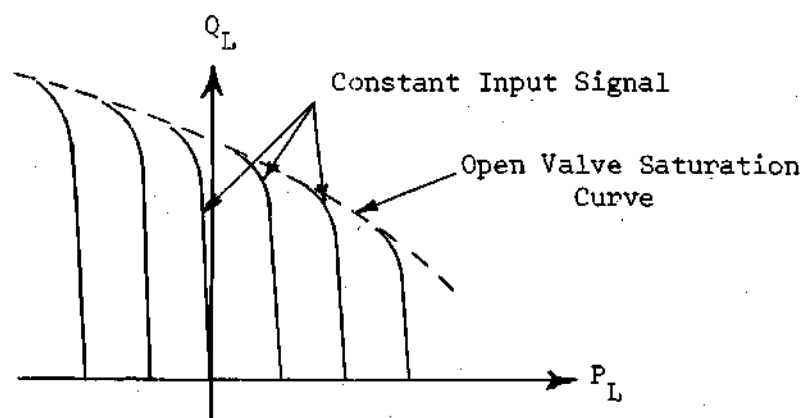


Figure 2. Typical Pressure-flow Curves

As was pointed out in reference (2), pressure compensated valves give a direct control of the pressure and have a response comparable to flow compensated valves; but, with rate feedback, a pressure compensated valve gives a superior step response and improved settling time. A pressure compensated valve, however, usually is not as stiff as its flow-control counterpart.

The Steady State Tests

In the pressure compensated valve system in Figure 9, the input was a current signal and the load pressure output was the difference between the upstream pressure (P_1) and the downstream pressure (P_2). Two types of steady state tests were made on the pressure compensated valves, plus a third test using no compensation.

With Torque Motor

In the first test a constant current signal was applied to sustain the torque motor, and the loading orifice was varied to obtain different load flows. Load pressure (P_L), load flow (Q_L), and input current (i) were recorded. These data are shown in Figure 10. In this first test the torque motor did not give a constant force-current relationship for all positions. This was due in part to the nonlinear magnetic spring force. Therefore, a second test was made to determine the same characteristics without using the torque motor.

Without Torque Motor

In the second test, the force input was established by hanging various weights over a pulley. These weights gave a pure force input to the system. The characteristics resulting from this improved input were

more vertical and were a better approximation to theory. In Figure 11 a comparison is made using the predicted curves and the actual data.

Without Pressure Compensation

Pressure compensation was eliminated in the third test where pressure and flow were recorded for various fixed positions of the slider. Both load flow and supply flow were recorded and are both shown in Figure 12. The results in that figure indicate that the load flow (Q_L) is always greater than or equal to the supply flow (Q_S). This is due to the transformer action of the variable jet pump. A high supply pressure and low supply flow are furnished to the variable jet pump, where they are transformed into a lower pressure and higher flow to the load. However, when the load pressure is sufficiently high, entrainment of the exhaust fluid in the variable jet pump ceases. This will tend to reverse the exhaust flow and close the check valve. When the load pressure exceeds that required to close the check valve, the supply flow and load flow must be equal considering no transformer action is taking place.

Variable Jet Pump Valve

The pressure compensated variable jet pump valve was built in two parts. The first part, the variable jet pump, was presented in Chapter I. The second part is the pressure feedback piston and the downstream variable orifice combination. This section was made at the Georgia Tech Experiment Station Shop and is shown in Figure 13. Pressure feedback is accomplished in this section by applying the upstream load pressure (P_1) to the left-hand area of the piston and simultane-

ously applying the downstream load pressure (P_2) to the right-hand area. This piston is connected directly to the variable jet pump so that an increase in P_1 or an increase in P_2 tends to close or open the variable jet pump, respectively. With piston areas of approximately 0.02 square inches, 20 pounds force from the torque motor was required for a load pressure of 1000 psi. The return flow from the load was metered through the variable spool orifice which had a normalized gain of $K_o = 5.12$. In Reference (1), page 71, it is explained that

$$K_o = \frac{C_d \ell (d/2)}{\pi \frac{D^2}{4}}$$

where D = diameter of VJP throat

ℓ = circumference of orifice

d = diameter of VJP slider cone

C_d = coefficient of discharge of the orifice

This variable orifice is necessary to provide the negative load pressure (P_2) and is used to control the load when slowing is desired. As the variable jet pump valve slider moves to close the variable jet pump, the variable orifice also closes, thus increasing P_2 and slowing the load.

Torque Motor

A model 106 torque motor was purchased from D. G. O'Brian Company having approximately .04 pounds per milliamp. gain with a six-watt power rating. Without any springs, this torque motor had a high nonlinear negative spring rate due to the magnetic attraction of the armature to

the stator. This was approximately compensated by a linear spring giving a small positive spring rate.

Instrumentation

The equipment used to record the steady state tests included two Helicoid pressure gauges which had an accuracy of 1/4 of 1 per cent. These gauges read the load pressures P_1 and P_2 , and were calibrated against a Model H7-1003 Martin-Decker pneumatic calibrator. The load flow was measured by a Vickers constant displacement hydraulic motor, Model No. AR-10007-BEL. The hydraulic motor speed was displayed on a Hewlett Packard Model No. 5233L electronic counter. This counter was counting the teeth on a 120-tooth gear using a Model 836 photo pickup made by Power Instruments Incorporated. The supply flow was read by a Schutte and Koerting Company 3.5 gpm. rotameter which was calibrated by the manufacturer for Esso Univis J43 hydraulic fluid (Military No. H-5606-B) at 100°F. This rotameter was located in the exhaust line because the supply pressure was too high. This arrangement assumes that the leakage is small so that the supply and exhaust flows are almost equal.

The preceding steady state tests were each conducted with a constant supply pressure of 1240 psi and an exhaust pressure of 240 psi. A description of the hydraulic supply system used for these tests is presented in Appendix A.

CHAPTER III

DYNAMIC CHARACTERISTICS

Dynamic characteristics are a measure of a system's ability to follow a command signal from the controller. In the tests presented here, a sinusoidal current was the command signal. The current signal frequency was varied, and the magnitude of the system response was recorded. A theoretical approach is presented before the actual system response is shown.

Theoretical Response

Each part of the system is explained as a separate unit. After the characteristics of each part are determined, they are placed in a block diagram for the total system.

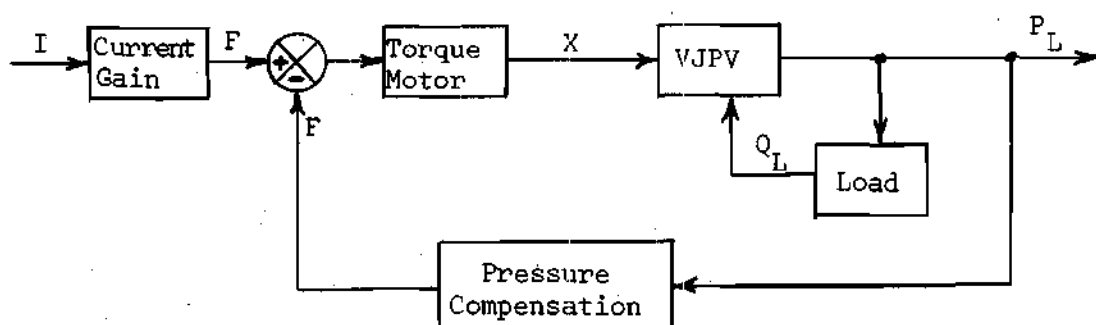


Figure 3. Block Diagram for Pressure Compensated Variable Jet Pump

Torque Motor

The torque motor is analyzed in two parts. First, a certain current input produces a force to the system. The ratio of normalized force to normalized current was

$$K_i = \frac{f}{i} = 1 \quad (2)$$

The second part of the torque motor analysis was its dynamic response. A frequency response test of the torque motor was conducted, showing that the torque motor reacted as a simple second-order system in the frequency range from 0.1 to 200 cycles per second. The transfer function using Laplace transforms was

$$\frac{F(S)}{X(S)} = \frac{7.2 \times 10^5}{S^2 + 1.1 \times 10^4 S + 7.2 \times 10^5} \quad (3)$$

If a substitution is made into the general form

$$\frac{F(S)}{X(S)} = \frac{1/M}{S^2 + \frac{D}{M} S + \frac{K}{M}} \quad (4)$$

The resulting values are

$$M = 1.39 \times 10^{-6}$$

$$D = 1.39 \times 10^{-2}$$

$$K = 1$$

Variable Jet Pump Valve

The variable jet pump valve also consists of two parts: the first is the variable jet pump, and the second is the downstream variable orifice.

Variable Jet Pump. The variable jet pump characteristics were obtained from Reference (1), page 30, and are formulated below.

$$p_1 = 2C_V q_S - (2 - \eta)q_S^2 - [2(2 - \eta)q_S + (2 - \eta - \psi)q_{eo}]q_S - q_L \quad (5)$$

$$q_S = \left(\frac{d}{D}\right)^2 [C_d(2X - X^2) + q_{NO}] \quad (6)$$

where

η = "diffusor" efficiency = .58

C_V = nozzle velocity coefficient = .97

ψ = exhaust flow momentum coefficient = .84

q_{NO} = leakage flow = 0

C_d = nozzle coefficient of discharge = .64

q_{eo} = linearized "average" exhaust flow = .35

These equations can be combined and linearized into the form*

$$\Delta p_1 = \Delta X f_1(X_{VJP}, Q_o) + \Delta q_L f_2(X_{VJP}, Q_o) \quad (7)$$

where

*See Appendix III for further explanation of derivations used in this section.

$$f_1(x_{VJP}, Q_o) = 2.19 + .793 x_{VJP} - 4.45 x_{VJP}^2 + \quad (8)$$

$$1.49 x_{VJP}^3 + 2.90 Q_o x_{VJP} - 2.90 Q_o$$

and

$$f_2(x_{VJP}, Q_o) = - .203 - .203 - .2.90 x_{VJP} + 1.45 x_{VJP}^2 \quad (9)$$

An operating point was chosen for both the theoretical and actual dynamic analysis. The normalized values for this point are

$$x_{VJP} = 0.12$$

$$x_{V0} = 0.28$$

$$Q_o = 0.343$$

$$P_o = 0.23$$

For this operating point

$$f_1(x_{VJP}, Q_o) = 1.35 \quad (10)$$

and

$$f_2(x_{VJP}, Q_o) = - 0.549 \quad (11)$$

Variable Orifice. The second part of the variable jet pump valve is the variable orifice, a simple spool valve which is characterized by the normalized equation for flow

$$q_L = K_O \times \sqrt{P_2 - P_E} \quad (12)$$

(K_O was defined in Chapter II)

This equation, like Equation (3), can be linearized into the form

$$\Delta p_2 = \Delta x f_3(X_{V0}, Q_O) + \Delta q_L f_4(X_{V0}, Q_O) \quad (13)$$

where

$$f_3(X_{V0}, Q_O) = - \frac{2 Q_O^2}{K_O^2 X_{V0}^3} \quad (14)$$

and

$$f_4(X_{V0}, Q_O) = \frac{2 Q_O}{K_O^2 X_{V0}^2} \quad (15)$$

This operating point for the variable orifice is the same as the one for the variable jet pump; however, the value of X is different because there was an underlap of $x = -0.16$. This operating point gives the values of

$$f_3(X_{V0}, Q_O) = - 0.405 \quad (16)$$

and

$$f_4(X_{V0}, Q_o) = 0.33 \quad (17)$$

A block diagram of these linearized systems is shown below where x and q_L were the input and p was the output.

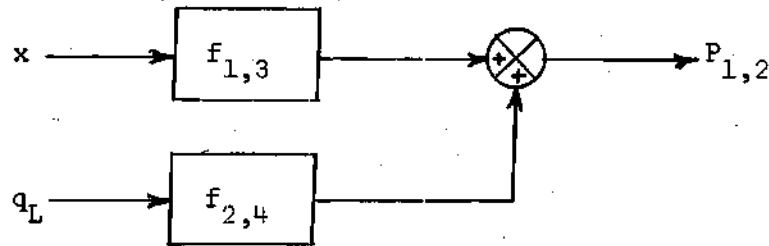


Figure 4. Linearized Variable Jet Pump or Variable Orifice Block Diagram.

The variable jet pump produces the upstream load pressure P_1 and the variable orifice produces P_2 . The difference in these pressures is the load pressure P_L . When the variable jet pump and variable orifice block diagrams are combined, the resulting arrangement is shown in Figure 5, appearing on the following page.

Load Orifice

The load is a simple orifice in which the pressure and the flow are related by a linear coefficient at the operating point.

$$K_L = \frac{1}{2} \frac{Q_o}{(\sqrt{P_o})^2} \quad (18)$$

therefore,

$$K_L = 0.745 \quad (19)$$

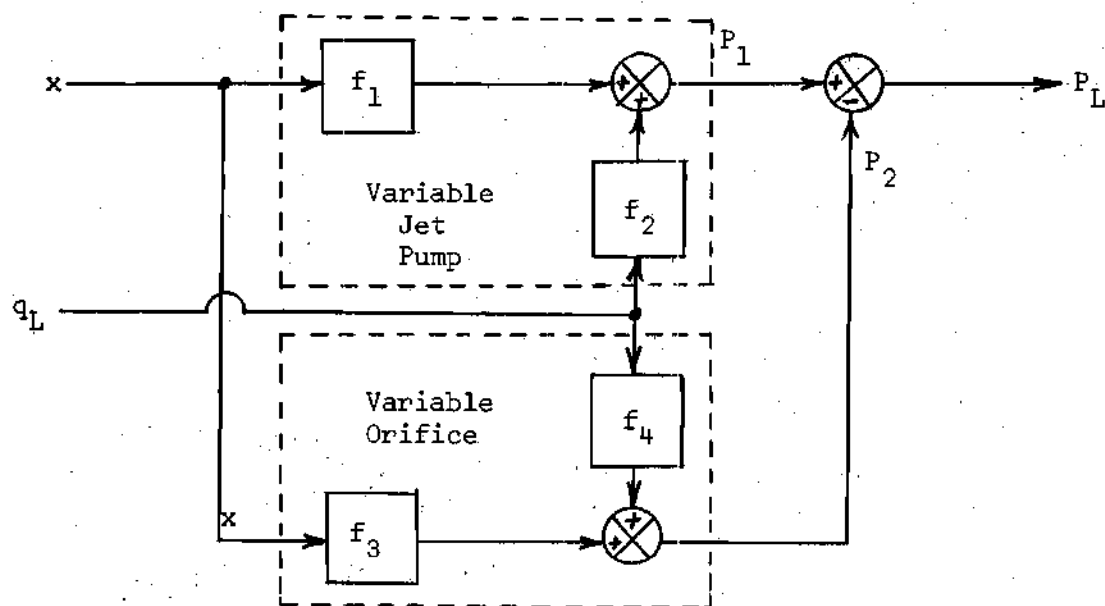


Figure 5. Combined Variable Jet Pump Valve Block Diagram

Pressure Compensation

In the compensating piston, a force is produced that is proportional to the load pressure by a factor equal to the piston area

$A = 0.02$ square inches. In normalized form, the value for K_F would be

$$\frac{(P_S - P_e)A}{K_{TM} \left(\frac{d}{2}\right)} = K_F = 1.115 \quad (20)$$

Composite System

Each transfer function of the block diagram shown in Figure 3 has been evaluated. When these transfer functions are substituted, a new block diagram shown in Figure 6 results. This block diagram

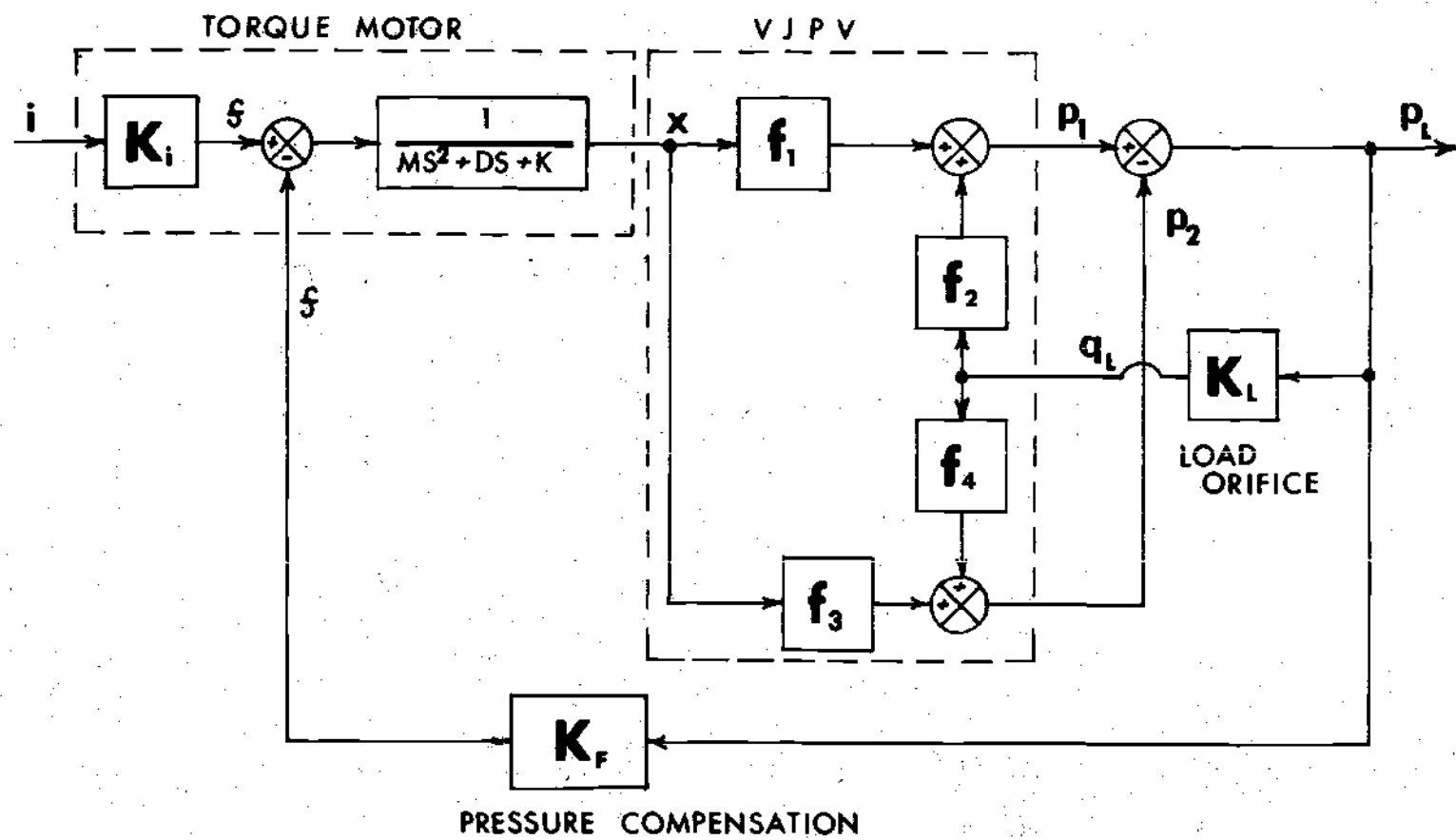


Figure 6. Composite System

be reduced to a simple second-order transfer function of the form

$$\frac{P(S)}{I(S)} = \frac{A}{S^2 + BS + C} \quad (21)$$

By substituting the values from the above analysis, the result is

$$\frac{P(S)}{I(S)} = \frac{806,000}{S^2 + S 13650 + 1,810,000} \quad (22)$$

This is a system with a natural frequency near 214 cycles per second and a damping ratio of approximately 1.02.

Assumptions

In the above analysis, certain assumptions were necessarily made. Some of these are:

1. There was incompressible flow throughout the system. This also means there was no air in the hydraulic fluid.
2. The transmission lines were rigid.
3. The variable jet pump gave a flat frequency response for all frequencies including these tests.
4. The "inertia effects" of the oil mass were small.

If one or more of these assumptions were proved to have an effect, they would tend to lower the system response. First, all hydraulic fluids are compressible. The bulk modulus of Univis J-43 is approximately 3×10^5 psi. The real problem involves the presence of air in the fluid in undissolved form. A graph in Reference (3)

indicates that if just 1 per cent of the air-fluid mixture is undissolved air, the bulk modulus would be reduced by a factor of 1/2 at 1000 psi, and by a factor of 9/10 at 200 psi. No provision was made to deaerate the fluid, although no bubbles could be observed in the flow-meter. Second, the transmission lines were made of steel and were also relatively short with rigid connectors. Third, the variable jet pump has no characteristic attenuation up to 300 cycles per second (1). Fourth, the effect of the mass of hydraulic oil on the system dynamic response is most evident in systems with long narrow lines from the control to the load (4). The mass of oil in the lines of the present system would theoretically have a resonant frequency greater than 20,000 cps. However, this value is proportional to the square root of the bulk modulus which is reduced considerably in the presence of undissolved air.

Actual Results

In the actual frequency test, the system was set up and run at the steady state operating point used in the above theoretical analysis. A sinusoidal current signal of approximately 200 ma. amplitude was the input. This signal was varied in frequency from 5 to 300 cycles per second, and the amplitude of the output pressure was recorded. A Bode plot of the magnitude of the response is shown in Figure 14. This curve shows a resonance frequency in the neighborhood of 70 cycles per second. The phase lag was approximately 90 near the peak, and approaching 180 at 200 cycles per second. These data are disappointing, especially when they are compared to a commercially-available Moog pres-

sure compensated servo valve (5). This valve is reported to have a natural frequency near 200 cycles per second.

There was also an unstable condition at high amplitude inputs and higher frequencies. Apparently the slider was not vibrating to its end points. The oscillations did not always cease when the input was turned off and had to be physically damped out. These oscillations had a frequency of approximately 200 cycles per second. At times when the system was under greatest stress, this unstable condition occurred spontaneously.

Instrumentation and Equipment

Special high frequency instrumentation was used in the dynamic tests. This instrumentation included two Statham PA-220TC strain gauge pressure transducers used to measure the load pressure. The two signals from the transducers were summed on a Dymec model DY-2460A amplifier with a gain of approximately 300. A Sanborn DCDT position transducer was employed to record the dynamic position of the slider. The input signal originated from a Hewlett Packard Model 202A low frequency function generator. The signal was amplified by an Inland Controls model 50A Hyband servo amplifier which was powered by a 28-volt Kepco model PRM28-7 D.C. power supply. Pressure, position, and current input signals were recorded from a Tektronics Type 555 dual beam oscilloscope. A line diagram for the equipment hookup is shown in Figure 15.

CHAPTER IV

CONCLUSIONS AND RECOMMENDATIONS

The goal of this work was to expand the application of the variable jet pump by building it into a system and studying the system's performance. The results were, in general, predictable and good. The most apparent system drawback, in the author's opinion, stemmed from using the torque motor to supply the force required to balance the feedback pressure. This one element, the torque motor, caused trouble in both the static and dynamic tests. In the static tests the torque motor caused the characteristic curves to be very nonlinear and sloped. This was, as discussed before, due to the inability to completely compensate for the negative magnetic spring force. In the dynamic tests the torque motor response appeared very similar to that of the system, only it had a break frequency of 135 cps.

The theoretical analysis in Chapter III showed that the torque motor response should have had only a small effect when using the high gain pressure feedback. However, it should be noted that in the system dynamic tests stiction was such that it required a minimum of 200 ma. peak-to-peak sinusoidal current to excite the system. This value of current is equivalent to ± 200 psi. when the operating point was only 230 psi. So, the assumptions concerning the small input signal and small motion of the torque motor are not completely valid. An obvious answer to this problem would be a high performance single-stage servo

valve to provide the force needed to balance the feedback pressure.

One of these valves made by Moog Servocontrols (6) can supply pressures up to 1000 psi. using less than 10 ma. and having a resonant frequency near 700 cycles per second.

The other area of doubt was the presence of undissolved air in the system. Using the "closed loop" supply system, any air present in the system at start-up was trapped in the system. Although the oil in the system was run from the reservoir for some time before any tests were conducted, it was evident that all the air was not removed.

In succeeding work with the variable jet pump, the problems mentioned above should be kept in mind. Areas of future study could include: observing the effects of cavitation on life, operation, and dynamic response; looking into practical upper and lower limits on size, pressure, and flows; changing the system in order to help mass production; and studying other areas of application using the variable jet pump in conjunction with fluid logic systems or other control systems.

APPENDIX I

HYDRAULIC SUPPLY SYSTEM

The hydraulic power supply for the system is shown in Figure 7. The high pressure pump supplying the pressure P_S was a Dennison series 600 pressure-regulated hydraulic pump. The smaller pump made by Roper Industries was used to charge the low pressure (exhaust) side of the system and to compensate for any leakage. Two one-gallon piston type accumulators made by Liquidonics Incorporated were used--one on the high pressure side was precharged to 750 psi, and one on the low pressure side of the system was precharged to 150 psi. The Sterlco flow control valve on the oil cooler maintained the oil temperature near 100°F.

The supply system had the capability of providing pressures with an upper limit of 5000 psi and flows up to 10 gpm. The return line could be operated from zero to 250 psi back pressure. Both pressures, P_S and P_E , could be maintained over the range of flows automatically. Variations due to disturbances damped out fairly fast.

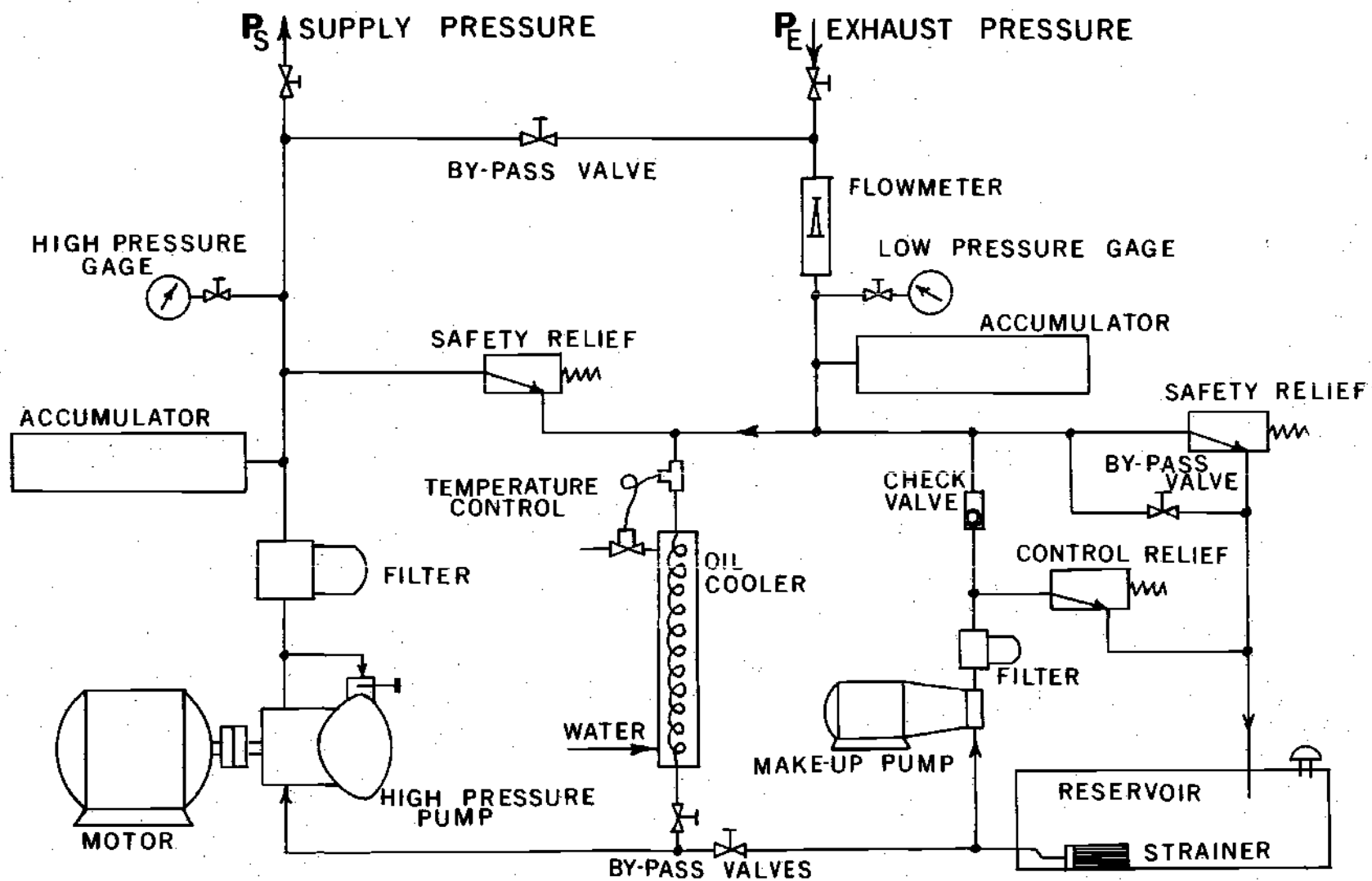


Figure 7. Hydraulic Power Supply System

APPENDIX II

ILLUSTRATIONS AND GRAPHICAL RESULTS

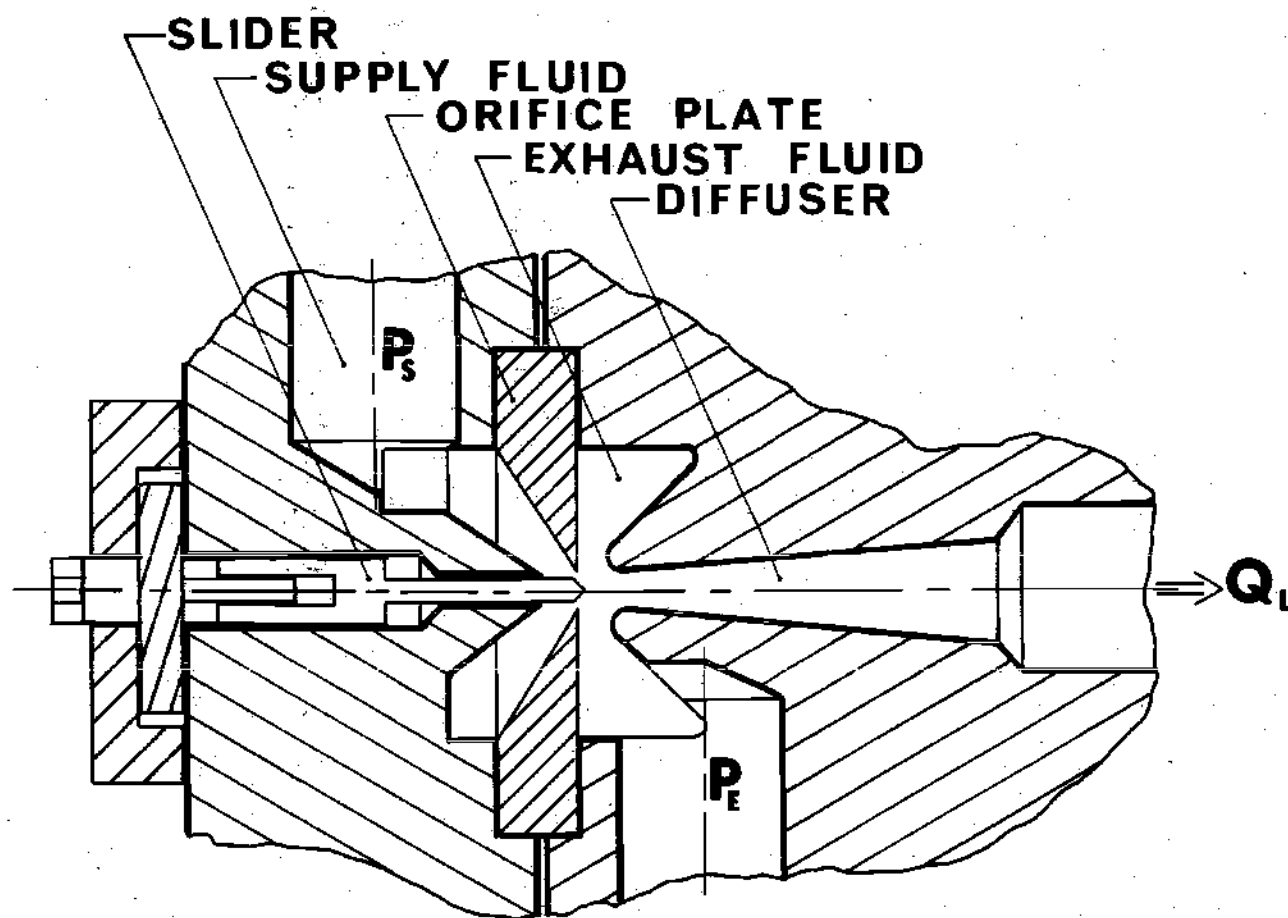


Figure 8. Variable Jet Pump Cross Section

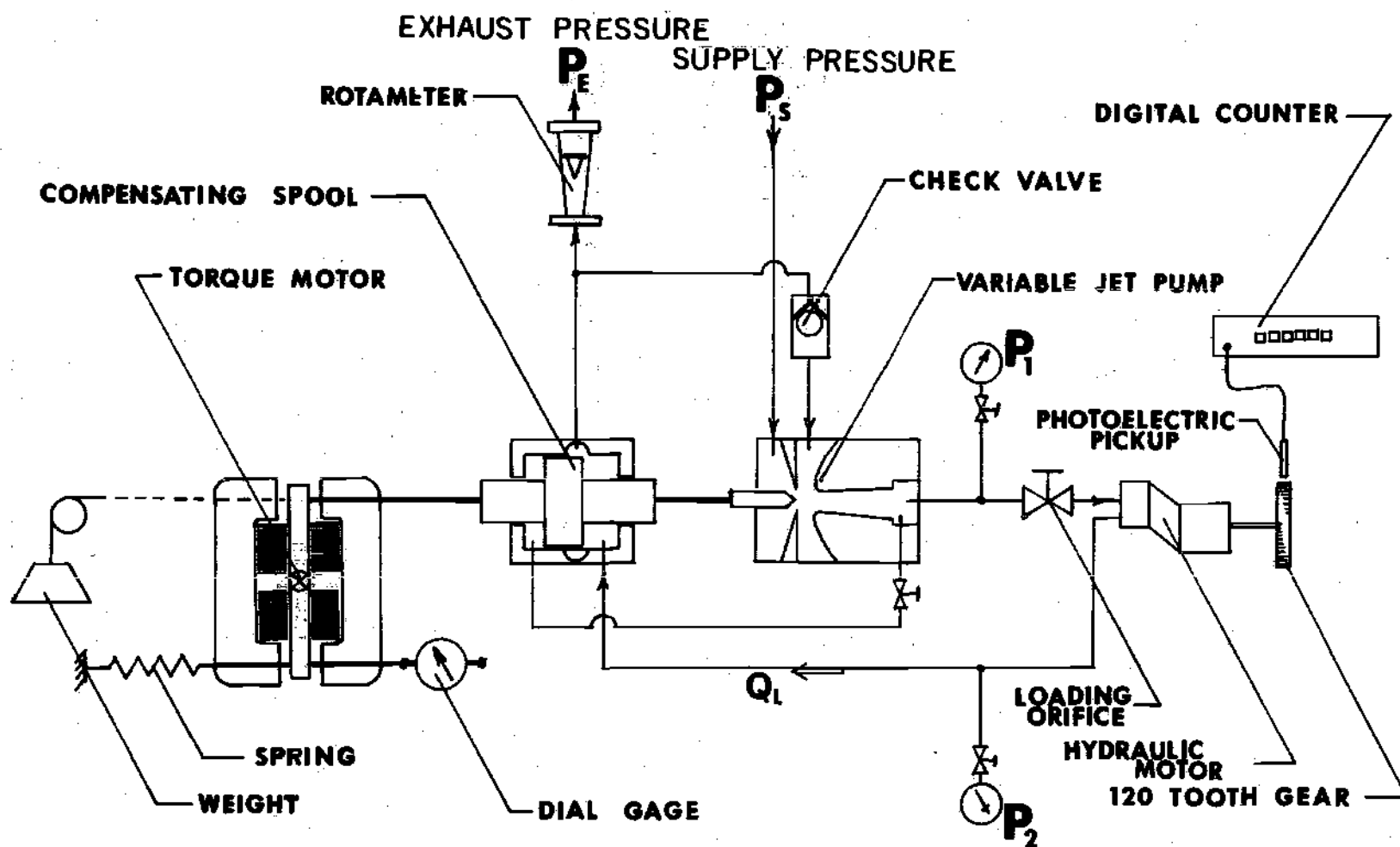


Figure 9. Two-way Variable Jet Pump Valve Arrangement

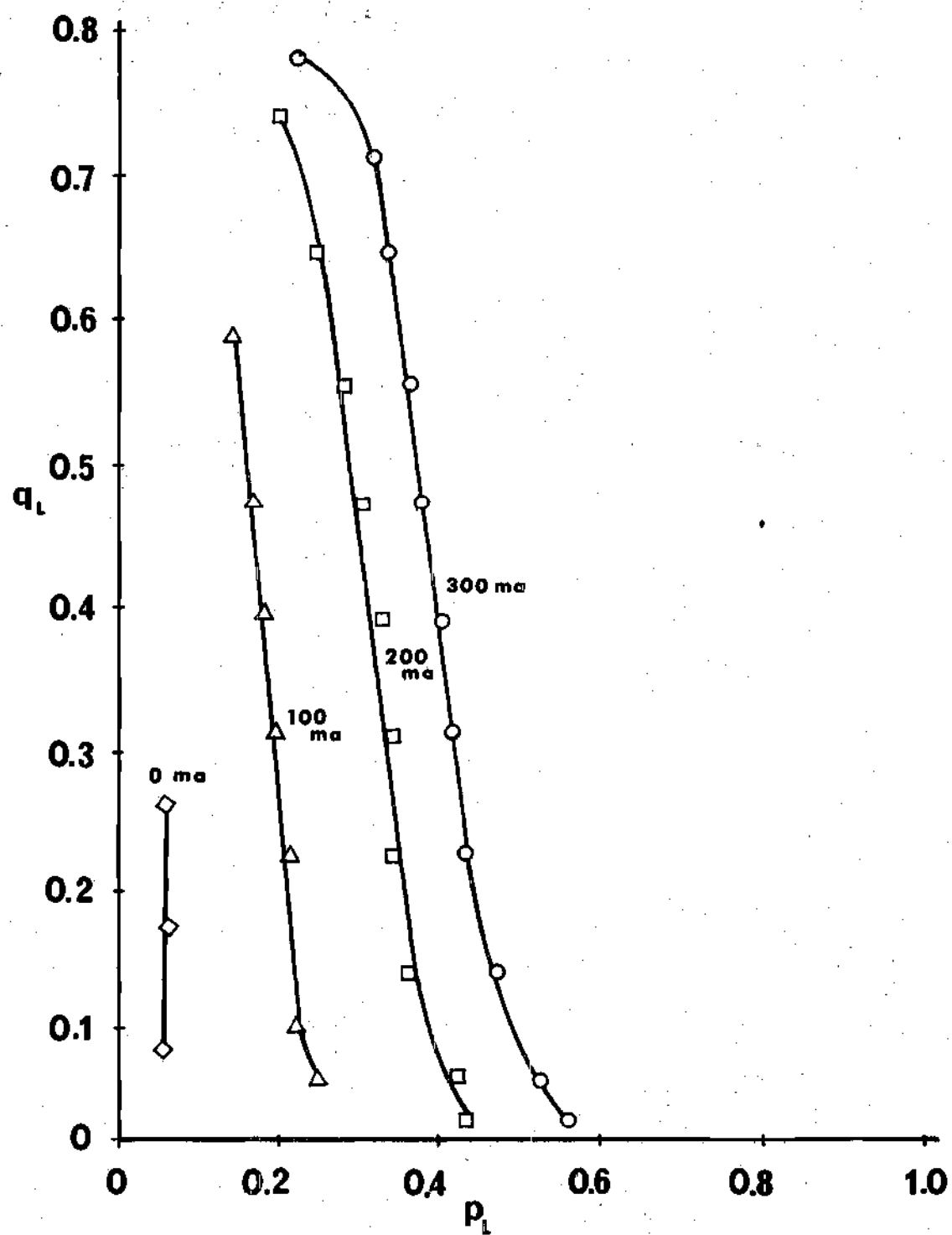


Figure 10. Variable Jet Pump Valve Characteristics with Torque Motor

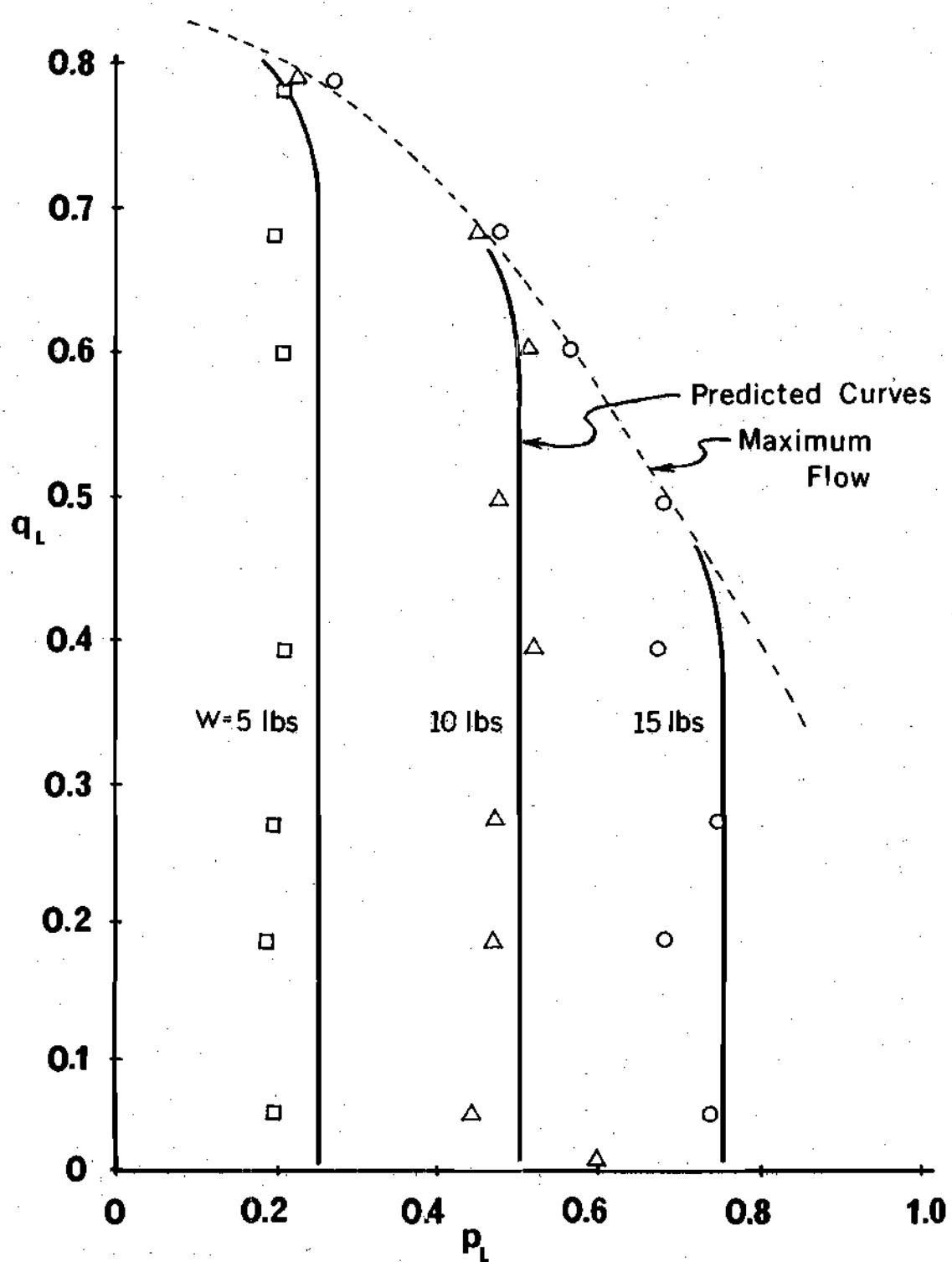


Figure 11. Variable Jet Pump Valve Characteristics without Torque Motor

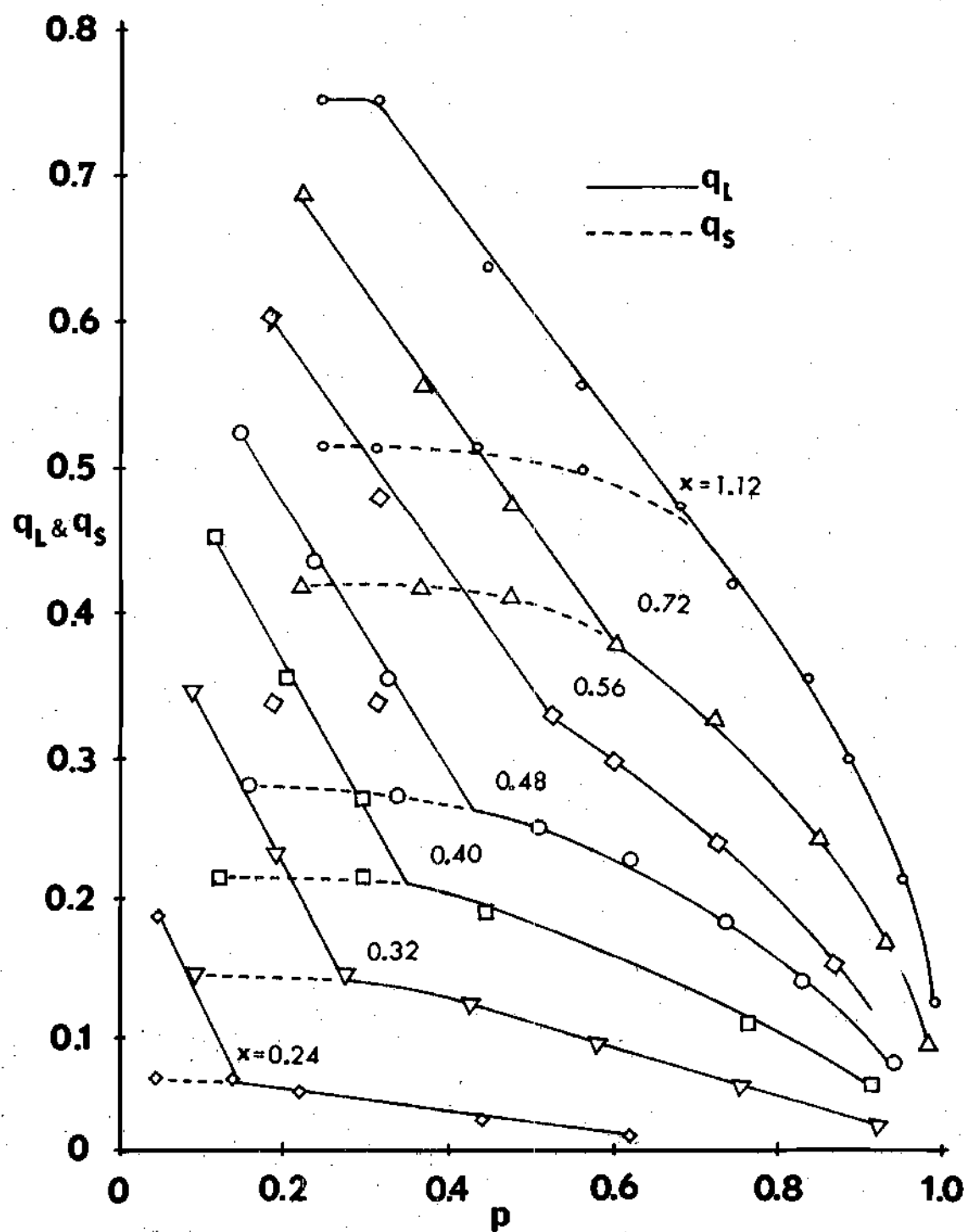


Figure 12. Variable Jet Pump Valve Characteristics without Pressure Compensation

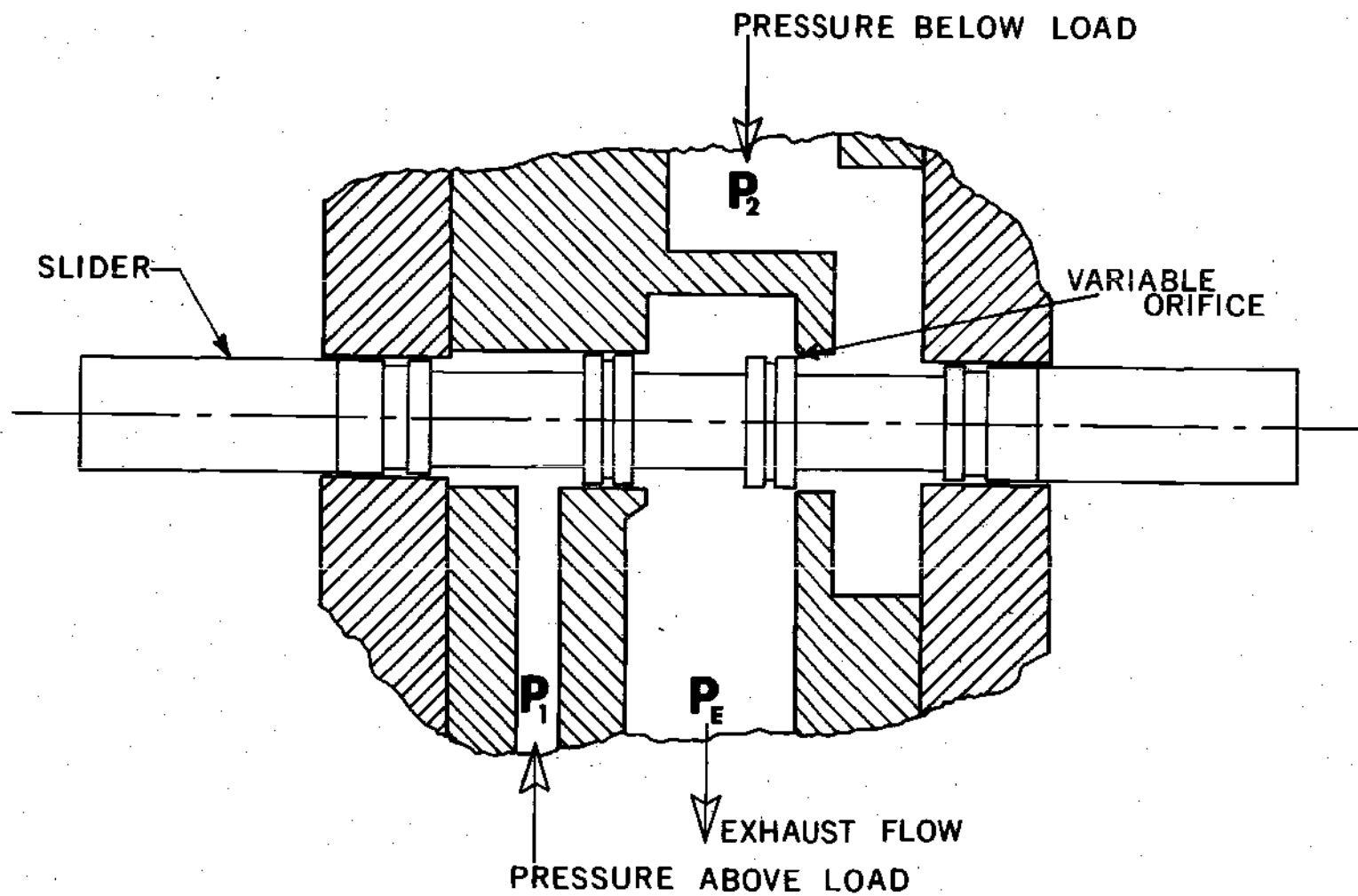


Figure 13. Pressure Compensating Spool and Downstream Orifice

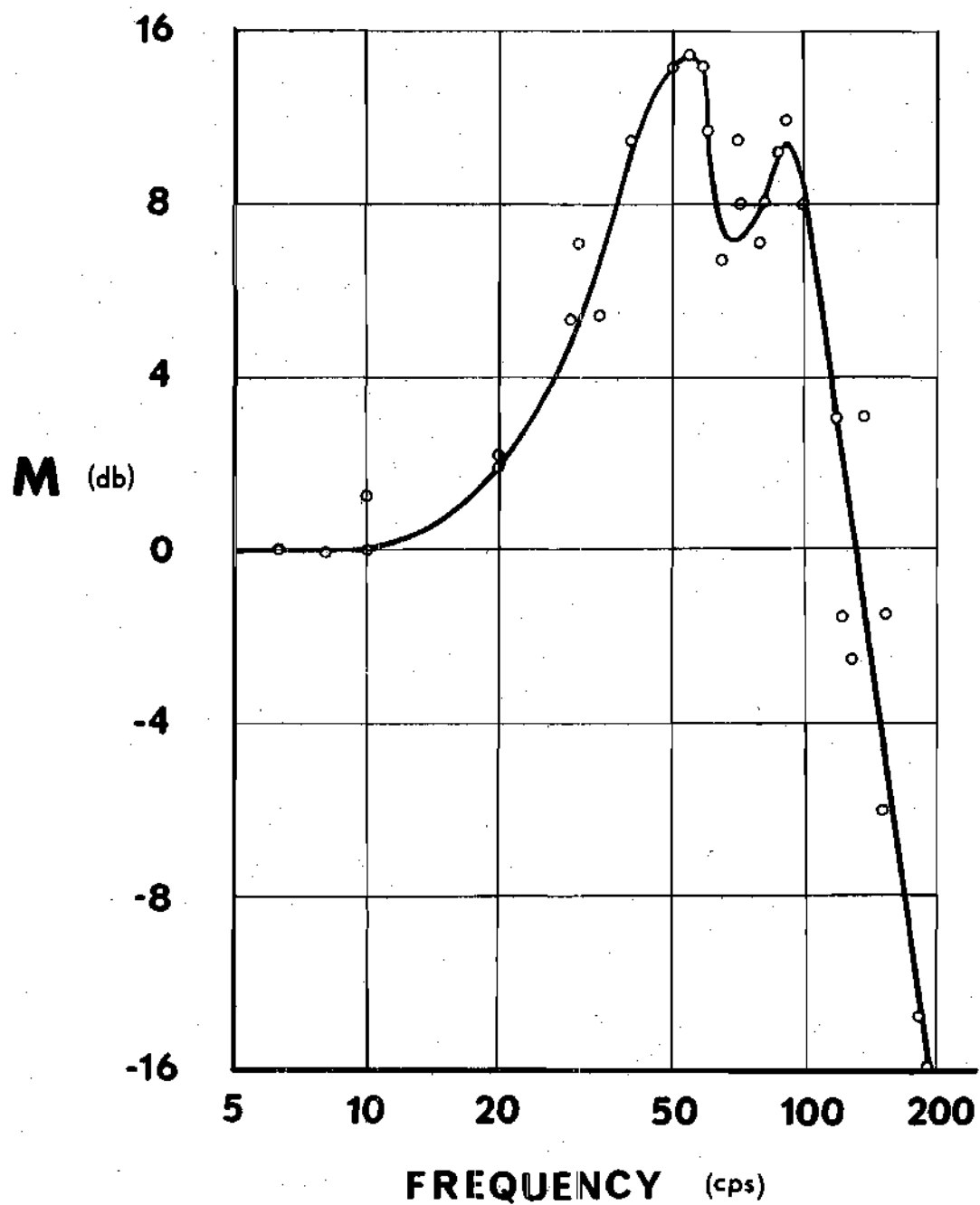


Figure 14. Variable Jet Pump Valve Frequency Response

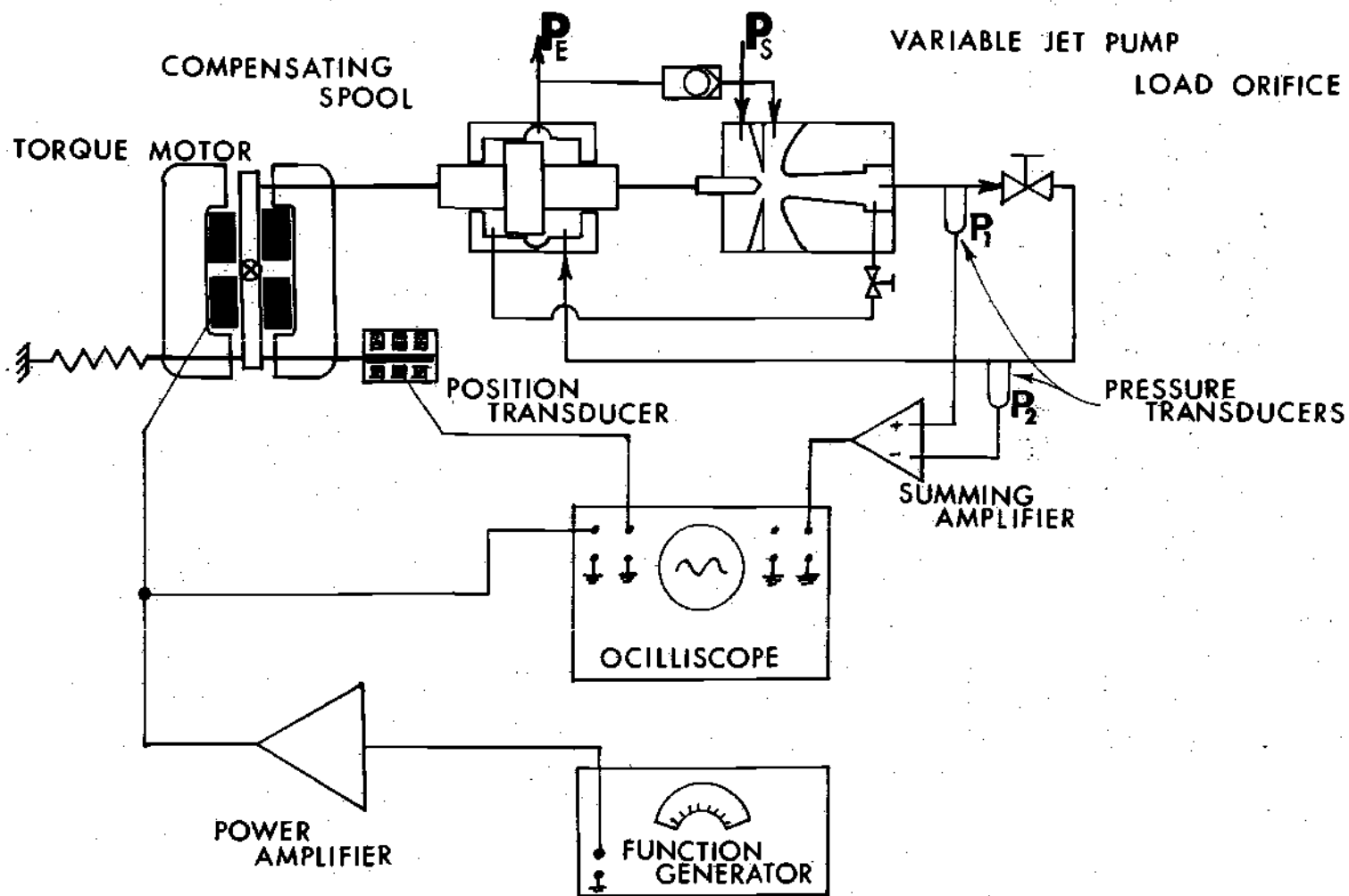


Figure 15. Variable Jet Pump Valve Dynamic Test Arrangement

APPENDIX III

CONSTANTS AND DERIVATIONS

Constants

A certain number of constants are used in this work without any explanation or values being given. The list included below is intended to provide these explanations.

<u>Symbol</u>	<u>Name</u>	<u>Value</u>
D	throat diameter	.07 inches
d	slider diameter	.0625 inches
A_T	throat area	.00385 in. ²
P_S	supply pressure	1240 psi.
P_E	exhaust pressure	240 psi.
ρ	density of J-43 hydraulic fluid at 98°F	$7.8 \times 10^{-5} \frac{\text{lbs sec}^2}{\text{in}^4}$
K_{TM}	torque motor spring constant	571 lbs/in
G_{TM}	torque motor current gain	.04 lbs/ma.
d/2	normalizing slider position	.03125 in.
$P_S - P_E$	normalizing pressure	1000 psi.
$K_{TM}(d/2)$	normalizing force	17.9 lbs.

<u>Symbol</u>	<u>Name</u>	<u>Value</u>
$A_T \sqrt{2/\rho (P_S - P_E)}$	normalizing flow	19.24 in ³ /sec
$\frac{K_{TM}(d/2)}{G_{TM}}$	normalizing current	447.5 ma.

The Torque Motor Transfer Function

The torque motor frequency response is shown in Figure 16. By inspection it can be seen that these data resemble the dynamic response of the second-order system with a break frequency of $\omega_n = 135$ cps. and a damping ratio of $\zeta = .65$. By substituting into the equation for the classical second-order transfer function

$$\frac{X(S)}{F(S)} = \frac{\omega_n^2}{S^2 + 2\zeta\omega_n S + \omega_n^2} \quad (23)$$

formula (3) is obtained

$$\frac{X(S)}{F(S)} = \frac{7.2 \times 10^5}{S^2 + 1.1 \times 10^4 S + 7.2 \times 10^5} \quad (24)$$

The "conservation of force" equation for a spring mass system can now be evaluated.

$$F = M\ddot{X} + D\dot{X} + KX \quad (25)$$

Laplace transforming the variables with initial conditions = 0

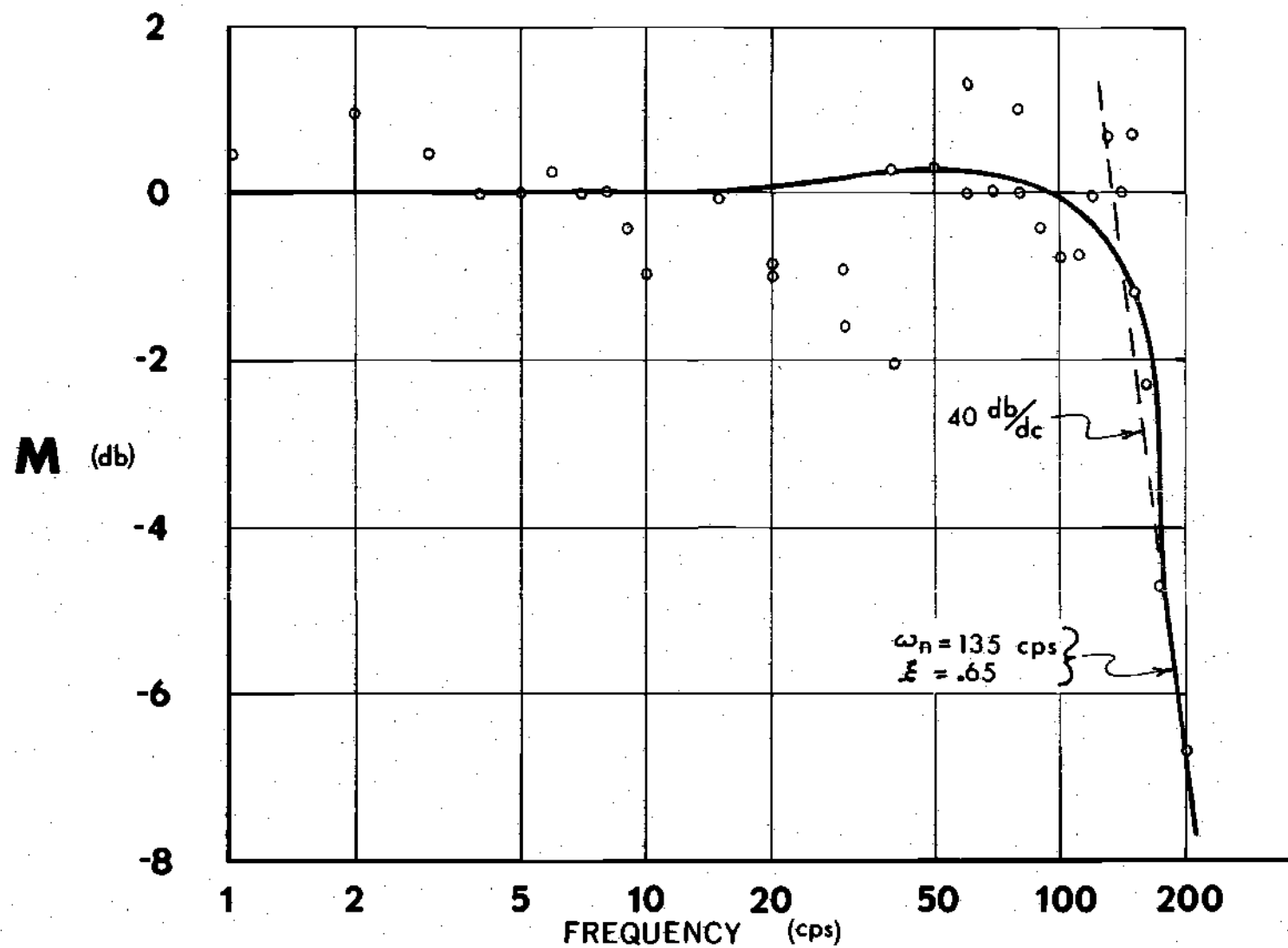


Figure 16. Torque Motor Frequency Response

$$F(S) = MS^2 X(S) + DSX(S) + KX(S) \quad (26)$$

or

$$\frac{X(S)}{F(S)} = \frac{1/M}{S^2 + \frac{D}{M}S + \frac{K}{M}} \quad (27)$$

Now, by evaluating Equations 24 and 26, the effective values for mass, damping, and spring constant are, respectively:

$$M = 1.39 \times 10^{-6}$$

$$D = 1.53 \times 10^{-2}$$

$$K = 1$$

Linearization of Equations

An equation of three variables $p = f(x, q)$ can be linearized using the Taylor series approximation. If there is a point where $P_0 = f(X_0, Q_0)$, and if for small disturbances from this point

$$|x - X_0| \leq |\Delta x| \quad (28)$$

and

$$|q - Q_0| \leq |\Delta q| \quad (29)$$

then the Taylor series is

$$f(x, q) = f(X_o, Q_o) + \sum_{j=1}^n \frac{1}{j!} \left[\Delta x \left. \frac{\partial}{\partial x} \right|_{X_o} + \Delta q \left. \frac{\partial}{\partial q} \right|_{Q_o} \right]^j f(x, q) + R_n \quad (30)$$

Now since Δx and Δq are small, it is assumed that all the terms of the series for $n \geq 2$ are very small and can be dropped. The resulting equation would be

$$f(x, q) = f(X_o, Q_o) + \Delta x \left. \frac{\partial}{\partial x} f(x, q) \right|_{X_o} + \Delta q \left. \frac{\partial}{\partial q} f(x, q) \right|_{Q_o} \quad (31)$$

If $\Delta p \equiv p - P_o$, and since $p = f(x, q)$ and $P_o = f(X_o, Q_o)$, then

$$\Delta p = \Delta x \left. \frac{\partial}{\partial x} f(x, q) \right|_{X_o} + \Delta q \left. \frac{\partial}{\partial q} f(x, q) \right|_{Q_o} \quad (32)$$

In the general linearized form

$$\Delta p = \Delta x f_a(X_o, Q_o) + \Delta q f_b(X_o, Q_o) \quad (33)$$

Equations for Variable Jet Pumps and Load Orifice

Equations 5 and 6 can be combined by substituting for q_s in Equation 5. The result is of the form $p_1 = f(x, q_L)$. This equation can be linearized as described above to obtain Equation 7.

$$p_1 = x f_1(X_{VJP}, Q_o) + q_L f_2(X_{VJP}, Q_o) \quad (34)$$

where f_1 and f_2 are the functions of X_{VJP} and Q_o after the partial

derivatives have been taken and the values for the constants from Equations 5 and 6 have been substituted.

Equation 12 can be rearranged to give

$$p_2 = \frac{q_L^2}{K_x^2} - p_E \quad (35)$$

which is of the form $p_2 = f(x, q_L)$ where p_E is a constant. Equation 35 now can be linearized to give Equation 13, 14, and 15.

The Load Orifice Constant

The load orifice constant was obtained by linearizing the flow equation

$$q = W\sqrt{p_L} \quad (36)$$

to the form

$$\Delta q_L = 1/2 \frac{W}{\sqrt{P_o}} \Delta p_L \quad (37)$$

However, at the operating point

$$W = \frac{Q_o}{\sqrt{P_o}} \quad (38)$$

Therefore, if the load orifice constant is defined as

$$K_L \equiv \frac{\Delta q_L}{\Delta p_L} \quad (39)$$

then

$$K_L = \frac{1}{2} \frac{Q_o}{(\sqrt{P_o})^2} \quad (40)$$

and at the operating point ($Q_o = 0.343$ and $P_o = 0.23$)

$$K_L = 0.745 \quad (41)$$

BIBLIOGRAPHY

1. Dickerson, Stephen L., *A Variable Fluid Transformer for Increasing Efficiency in Hydraulic Control Systems*, Sc.D. Thesis, Massachusetts Institute of Technology, June, 1965..
2. Blaiklock, Paul M., *Hydraulic Position Control System*, M.S. Thesis, Massachusetts Institute of Technology, May, 1965.
3. Smith, L. H.; Peeler, R. L.; Bernd, L. H.; "Hydraulic Fluid Bulk Modulus--Its Effect on System Performance and Techniques for Physical Measurement," *16th National Conference on Industrial Hydraulics*, Vol. X, 1956, p. 184.
4. Healey, A. J., "Effect of Oil Inertia on Resonant Frequency of Hydraulic Drives," *Control*, April, 1966, pp. 181, 182.
5. Thayer, W. J., "Transfer Function for Moog Servovalves," *Moog Servocontrols, Incorporated*, Bulletin 103, revised 1965, p. 4.
6. Williams, L. J., "High Performance Single-Stage Servovalve," *Moog Servocontrols, Incorporated*, Bulletin 106, May, 1965.